Current-voltage dynamics of multi-junction CPV modules under different irradiance levels

Eduardo F. Fernández*, Juan P. Ferrer-Rodríguez, Florencia Almonacid and Pedro Pérez-Higueras

Centro de Estudios Avanzados en Energía y Medio Ambiente (CEAEMA), IDEA Solar Energy Research Group, Universidad de Jaén, Las Lagunillas Campus, Jaén 23071, Spain

**Corresponding author: fenandez@ujaen.es, +34 9543213520*

Abstract. The current-voltage output of concentrator photovoltaic (CPV) modules shows a complex behaviour under irradiance variations due to the use of multi-junction solar cells and optical elements. The single exponential model (SEM) relates the I-V curve of a PV device and its five characteristic parameters. Hence, it is fundamental to understand the dependence of the SEM model and I-V parameters of CPV modules with irradiance. In this paper, two samples of concentrator modules were characterized under fully controlled conditions by using a CPV solar simulator for light intensities within 700-1000 W/m^2. Results show that the photo-generated current increases linearly with irradiance, the diode ideality factor and saturation current present a stable behaviour under irradiance variations while the parasitic resistances, i.e. series and shunt, trend to decrease as the intensity increases. In addition, different approximations are carried out in the SEM model equation to explain the dependence of the performance of the concentrators with light intensity. Finally, the prediction of the I-V curves and key electrical parameters from reference values is discussed. Results show a good fitting of the I-V curves until 750 W/m^2 and a high accuracy in the estimations of the electrical parameters with a MAPE lower than 1.2%, a MRE within 1% and a R^2 equal of higher than 0.9.

Keywords: I-V characteristics, SEM model parameters, light intensity variations, multi-junction CPV modules.

1. Introduction

Concentrator photovoltaics (CPV) is considering as one of the most promising research avenues to reduce the cost of solar electricity and for large scale implementation (Talavera, et al., 2016; Talavera, et al., 2017). The CPV module is the fundamental unit of this technology to convert the non-concentrated sunlight into electricity. Nowadays, these modules are largely based on multi-junction (MJ) solar cells made up of several p-n junctions interconnected in series, usually a GaInP/GaInAs/Ge structure, to improve the absorption of the spectral irradiance (Cotal, et al., 2009; Fernández, et al., 2015a). The most widely used optical configuration is based on a primary optical element (POE) and a secondary optical element (SOE) per receiver (Shanks, et al., 2016). The aim of the POE, usually a Fresnel lens, is to collect and concentrate the direct light received from the sun (Xie, et al., 2011). On the other hand, the SOE, e.g. pyramid, CPC, SILO, etc., is intended to homogenize the luminous power on the solar cell surface and to improve the acceptance angle of the system (Victoria, et al., 2009). A passive cooling mechanism for avoiding overheating of the solar cells consisting of a flat back plate or finned heat-sink is used in the majority of the cases due to its simplicity and reliability (Micheli, et al., 2016; Rodrigo, et al., 2014).

The assembly of the elements above makes the electrical performance of CPV technology more complex and inherently different than conventional photovoltaics (PV) (Rodrigo, et al., 2013). Hence, important efforts have been made within last years to analyse the behaviour and to develop models tailored to the special features of this technology at cell (Theristis & O'Donovan, 2015; Fernández, et al., 2013a; Domínguez, et al., 2010), module (Fernández, et al., 2013b; Theristis, et al., 2017; Steiner, et al., 2015) and system level (Fernández, et al., 2015b; Kim, et al., 2013; Strobach, et al., 2015). This is crucial to gain a better understanding of the current-voltage output of concentrator devices as a function of the relevant input parameters, and therefore, to promote the market expansion of CPVs (Kurtz, et al., 2015; Leloux, et al., 2014; Fernández, et al., 2016a).

The single exponential model (SEM) relates the I-V curve of a PV device and its five characteristic parameters, namely, the photo-generated current, the diode saturation current, the diode ideality factor, the series resistance and the shunt (or parallel) resistance. The extraction and study of the SEM model parameters of PV devices have been under study for decades (Cotfas, et al., 2013; Ciulla, et al., 2014; Humada, et al., 2016; Li, et al., 2013; Li, et al., 2016; Ghani, et al., 2014). Last years, several authors have also applied different methods for extracting the five parameters of multi-junction CPV devices (Segev, et al., 2012; Ben Or & Appelbaum, 2013; Appelbaum & Peled, 2014; Almonacid, et al., 2016; Fernández, et al., 2016b). A semi-empirical method was applied to extract the parameters of InGaP/InGaAs/Ge solar cells under different concentrations and temperatures (Segev, et al., 2012). The Newton-Raphson method, the Levenberg-Marquardt method combined with Lambert-W function and a Genetic-Algorithm have been applied to the same structure under different concentration levels (Ben Or & Appelbaum, 2013; Appelbaum & Peled, 2014). More recently, numerical and analytical methods have been applied for the electrical characterization of a whole CPV module under real working conditions (Almonacid, et al., 2016; Fernández, et al., 2016b; Ghani, et al., 2017).

The direct irradiance is the main driver of the current-voltage output of CPV systems (Fernández, et al., 2013c). Because of this, it is fundamental to investigate the behaviour of the parameters of the SEM model and the I-V characteristics of concentrator modules as a function of this variable. However, only few studies, and mainly at cell level, have been conducted regarding the dependence of these magnitudes (Ben Or & Appelbaum, 2014; Khan, et al., 2014). Nevertheless, the dynamics of the current-voltage characteristics of CPV modules cannot be completely understood from the simply analysis of the concentrator cells employed. First, the use of optical devices could affect the uniformity over the solar cell surface, and therefore, the I-V characteristics of the concentrator (Baig, et al., 2012). Second, the interconnection of several receivers produces optical and electrical mismatches that could modify the performance of the system with light intensity (Rodrigo, et al., 2016; Peharz, et al., 2011). Finally, the wiring among the cells is expected to produce additional series resistance losses that could affect the evolution of the electrical characteristics with light intensity.

Bearing the above in mind, this paper aims to analyse and elucidate the behaviour of the SEM model and I-V parameters of multi-junction CPV modules with irradiance variations under fully controlled conditions. To the knowledge of the authors, this has not been addressed in any previous research work and is, therefore, still pending. In order to achieve this issue, two different CPV modules were characterized under laboratory controlled conditions by using the Helios 3198 CPV solar simulator for light intensities within 700-1000 W/m^2. Based on the experimental data, the SEM model parameters of the modules are extracted and their dependence with intensity discussed in relation to the physical properties of the multi-junction solar cells. Based on the extracted values, different approximations are carried out in the I-V characteristic equation to explain the electrical performance of the concentrators under irradiance variations. The accuracy in the modelling of the I-V curves and key electrical parameters with irradiance from the measured and extracted parameters at reference conditions is also investigated. The final goal is to contribute to the understanding and modelling of the performance of CPV modules as a function of the input direct irradiance.

2. Materials and experimental procedure

To carry out this study, two samples of commercial CPV modules from different manufactures have been selected i.e. module A and B. Both modules are based on triple-junction lattice-matched GaInP/GaInAs/Ge solar cells. The primary optics of the modules consists of point-focus flat Fresnel lenses. The module A uses silicone-on-glass (SoG) lenses, while the module B uses poly(methylmethacrylate) (PMMA) lenses. The modules also include a secondary optics based on refractive truncated pyramids made up of glass. The geometric concentration of the modules is 500x, module A, and 820x, module B. Both concentrators use a passive cooling mechanism to remove the heat generated by the cells. The cooling system of the module A is based on aluminium finned heat-sinks, while is based on a simple aluminium flat back plate for the module B. Additional information about the main characteristics of each module can be found in Table 1. In addition, Table 2 shows the rated values of the main electrical parameters of the two concentrators under reference conditions. The features of the modules selected represent the most wide-spread multi-junction concentrator PV system nowadays. Because of this, it is worth mentioning that the conclusions of this work can be considered representative of the current CPV technology (Rodrigo, et al., 2015).

Parameter	**Module A**	**Module B**
Geometric concentration	500x	820x
Primary optics	silicone-on-glass (SoG)	poly(methylmethacrylate) (PMMA)
Lens area	23.9 cm x 23.9 cm = 571 cm^2	20 cm x 20 cm = 400 cm^2
F-number	~ 0.90	~ 0.80
Secondary optics	refractive pyramid	refractive pyramid
Type of solar cells	lattice-matched GaInP/GaInAs/Ge	lattice-matched GaInP/GaInAs/Ge
Number of solar cells	6	25
Area of solar cells	~ 1 cm^2	~ 0.5 cm^2
Bypass diodes	1 per cell	1 per cell
Cooling type	passive (finned heat-sink)	passive (flat heat-sink)
Number of fins	10	-
Length of fin	9 cm	-

Table 1. Main features of the multi-junction concentrator PV modules used to carry out this study.

Parameter	**Module A**	**Module B**
I_{sc} (A)	5.84	4.29
I_{mpp} (A)	5.55	4.00
V_{oc} (V)	18.9	77.5
V_{mpp} (V)	16.8	68.3
FF (%)	84.5	82.2
η (%)	27.3	27.4

Table 2. Rated values of the main electrical parameters of the concentrator PV modules used in this study obtained with the Helios 3198 CPV solar simulator at the CEAEMA in the University of Jaen at 1000 W/m^2, spectral irradiance similar to AM1.5D reference spectrum, SMR (top/mid) = 1 ± 0.05 and room temperature of 25ºC ± 0.5ºC.

The multi-junction CPV modules were tested with the Helios 3198 solar simulator from Solar Added Value Company at the Centro de Estudios Avanzados en Energía y Medio Ambiente (CEAEMA) of the University of Jaen. This solar simulator uses a Xenon flash lamp for simulating the solar radiation and a parabolic mirror as a collimator. The spectral irradiance distribution is close to the AM1.5D reference spectrum, and the collimation angle is around ± 0.3º. Hence, this set-up represents a useful tool for the electrical characterization of CPV modules and systems under controlled conditions, see Figure 1. Additional detailed information about the features of the simulator can be found in (Domínguez, et al., 2008).

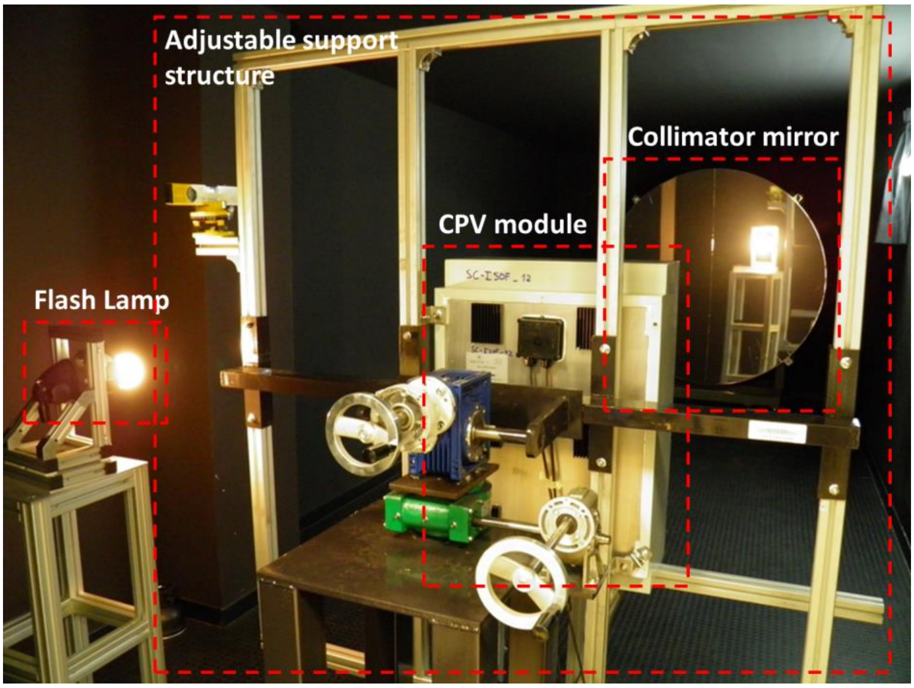

Figure 1. Photo of the Helios 3198 CPV solar simulator at the Centro de Estudios Avanzados en Energía y Medio Ambiente (CEAEMA) of the University of Jaen.

The modules were mounted on the support structure of the solar simulator. After that, the Fresnel lenses were cleaned and examined to avoid any distortion of the data caused by soiling or damaged optical elements. Later on, the modules were aligned to the continuous light, a halogen lamp located in the centre of the Xenon flash tube, by changing the azimuth and elevation angles of the adjustable support structure to diminish the possible effect of optical mismatches. The correct alignment of both systems is later verified by measuring the acceptance angle profile of the CPV modules in steps of around 0.15º by using the adjustment controls of the structure, see Figure 2.

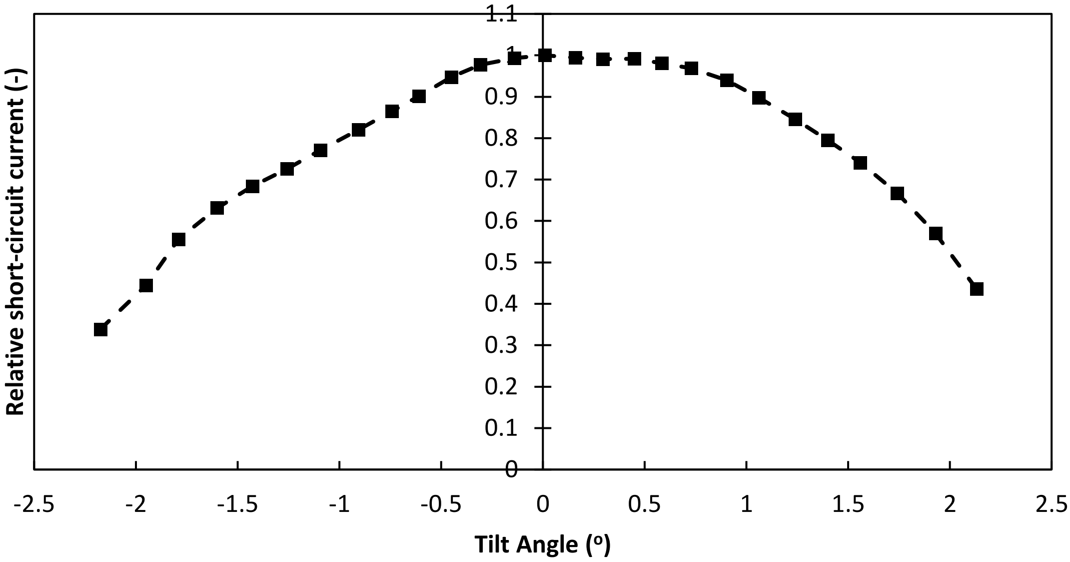

Figure 2. Acceptance angle profile of the CPV module A measured with the Helios 3198 CPV solar simulator at the CEAEMA in the University of Jaen at 1000 W/m^2, spectral irradiance similar to AM1.5D reference spectrum, SMR (top/mid) = 1 ± 0.05 and room temperature of 25ºC ± 0.5ºC. The optimum alignment is considered at the point 0 of the *x*-axis.

The modules were tested under light intensities from 700 to 1000 W/m^2, see Figure 3, which can be considered as a representative range of irradiance under actual conditions (Soria-Moya, et al., 2015). Each I-V curve was measured in steps of 50 W/m^2 by measuring a set of 20-25 current-voltage points spread relatively uniformly excepting in the "knee" of the curves, where a more density of measurement points was fixed. The room temperature was maintained at 25 ± 0.5ºC to avoid thermal effects in the results (Peharz, et al., 2011). Also, the Spectra Matching Ratio (SMR) (Domínguez, et al., 2013) for the top and middle subcells was monitored through the measurements of component cells from Solar Added Value Company with an equivalent structure than the MJ solar cells of the modules:

$$SMR\ (top/mid) = \frac{I^{c.c.}_{sc,top}}{I^{c.c.}_{sc,top,ref}} \frac{I^{c.c.}_{sc,mid,ref}}{I^{c.c.}_{sc,mid}} \qquad (1)$$

where $I^{c.c.}_{sc,top}$ and $I^{c.c.}_{sc,mid}$ are, respectively, the measured short-circuit currents of the top and middle components cells; the subscript "ref" refers to the values at reference conditions. This index has been recorded to ensure the adequate input spectrum for each light intensity due to the high spectral sensitivity of CPV modules caused by the use of multi-junction solar cells made up of various subcells with different band gaps (Fernández, et al., 2014; Fernández, et al., 2016c). The value of SMR (top/mid) was kept constant at 1 ± 0.05 for all the irradiance values, so that, the spectral effects are not expected to play an important role in the results (Muller, et al., 2015; Theristis, et al., 2016; Fernández, et al., 2015c).

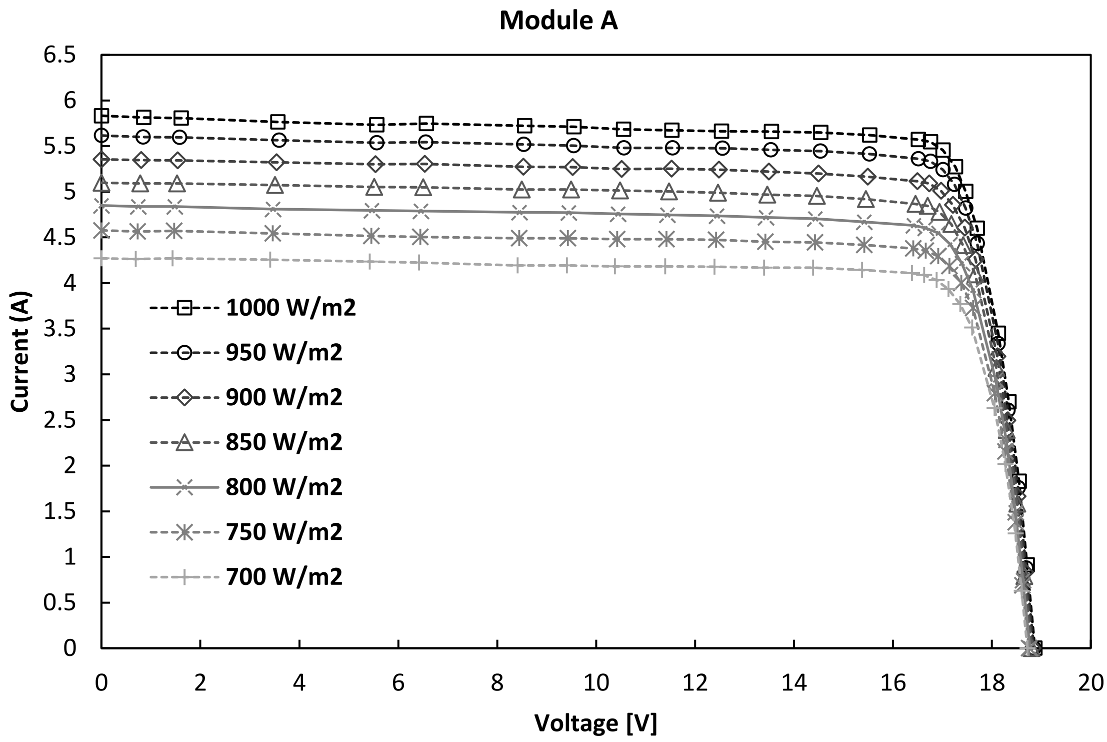

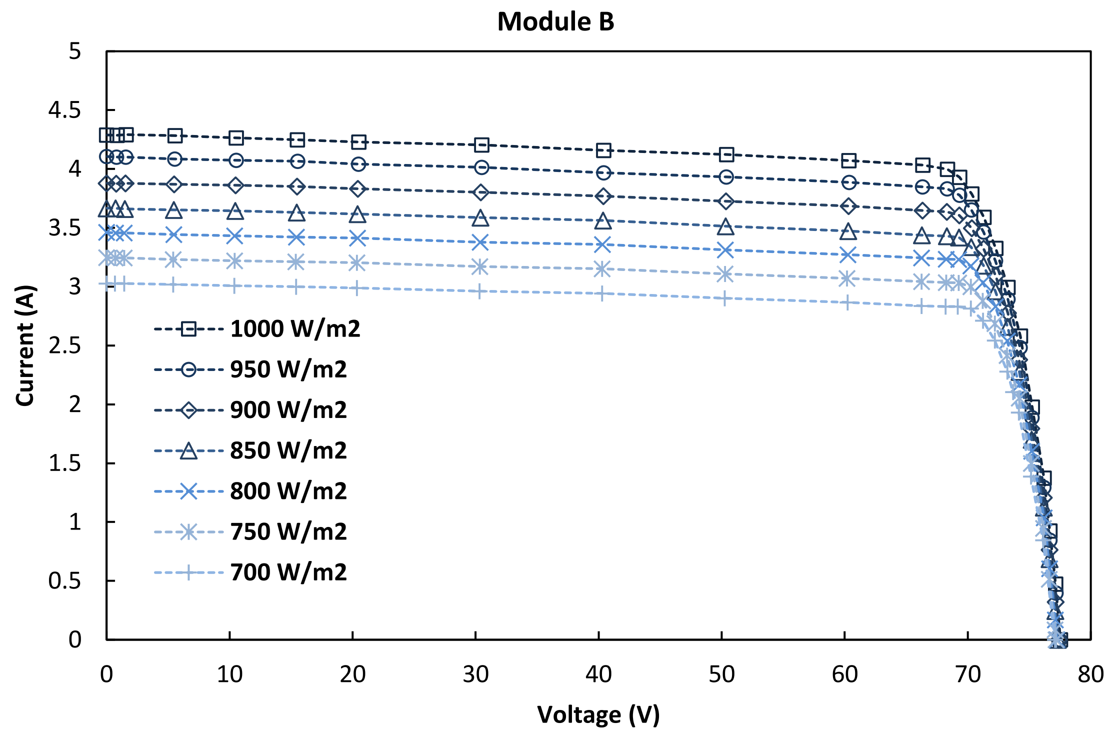

Figure 3. Current-voltage curves of the CPV modules used in this study measured with the Helios 3198 CPV solar simulator at irradiance levels within 700-1000 W/m^2, spectral irradiance similar to AM1.5D reference spectrum, SMR (top/mid) = 1 ± 0.05 and room temperature of 25ºC ± 0.5ºC.

3. Dependence of SEM model parameters with irradiance

In this section, first, the methodology used to extract the parameters of the SEM model is described and experimentally validated. After that, the impact of irradiance changes on the extracted parameters is discussed.

3.1. Methodology

The equivalent circuit shown in Figure 4 has recently demonstrated to be valid for the electrical characterization of multi-junction CPV modules (Almonacid, et al., 2016). Based on this circuit, the relation between the parameters of a concentrator module and its current-voltage electrical output can be expressed by the so-called single exponential model (SEM) as:

$$I = I_{ph} - I_o \left(\exp\left(\frac{V+IR_s}{mV_T}\right) - 1\right) - \frac{V+IR_s}{R_{sh}} \quad (2)$$

where I_{ph} is the photo-generated current, I_o is the diode saturation current, m is the diode ideality factor, R_s is the series resistance and R_{sh} is the shunt (or parallel) resistance of the modules. V_T in Equation (1) is defined as the thermal voltage, given by $V_T = kT/q$; being k the Boltzmann constant with a value of 1.38E-23J/K and q the elementary charge with a value of 1.60E-19C.

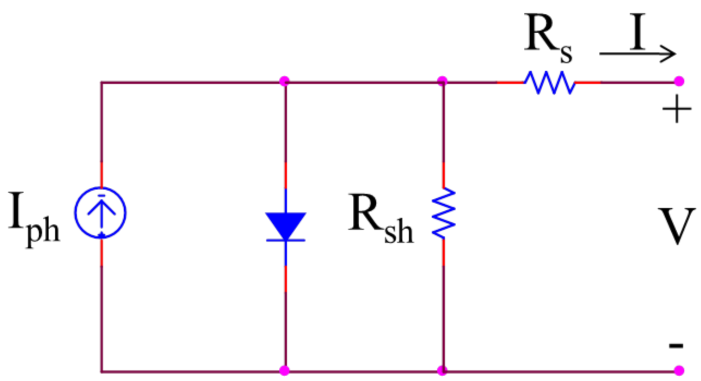

Figure 4. Equivalent circuit of the single exponential model of a photovoltaic device.

The five parameters of Equation (2) can be extracted from the measured I-V characteristics of the photovoltaic device under study. Several methods for extracting the five parameters of the SEM model for the electrical characterization of multi-junction CPV modules were evaluated in (Fernández, et al., 2016b). Among the different approaches analysed, the method of Phang et al. (Phang, et al., 1984) has been selected in this study due to its accuracy and simplicity. First, the initial values of R_{so} and R_{sho} are estimated by performing a linear fit of the I-V curve around the open-circuit voltage and the short-circuit current as:

$$R_{so} = -\left(\frac{dV}{dI}\right)_{V=V_{oc}} \quad (3)$$

$$R_{sho} = -\left(\frac{dV}{dI}\right)_{I=I_{sc}} \quad (4)$$

After that, the parameters of Equation (1) are estimated from the measure values of I_{sc}, V_{oc}, I_{mpp}, V_{mpp}, R_{so} and R_{sho} according to:

$$I_{ph} = I_{sc}\left(1 + \frac{R_s}{R_{sh}}\right) + I_o\left(\exp(\frac{I_{sc}R_s}{mV_T}) - 1\right) \quad (5)$$

$$I_o = \left(I_{sc} - \frac{V_{oc}}{R_{sh}}\right)\exp(-\frac{V_{oc}}{mV_T}) \quad (6)$$

$$m = \frac{V_{mpp}+R_{so}I_{mpp}-V_{oc}}{V_T\left[ln\left(I_{sc}-\frac{V_{mpp}}{R_{sh}}-I_{mpp}\right)-ln\left(I_{sc}-\frac{V_{oc}}{R_{sh}}\right)+\frac{I_{mpp}}{I_{sc}-\frac{V_{oc}}{R_{sh}}}\right]} \quad (7)$$

$$R_s = R_{so} - \frac{mV_T}{I_o}\exp(-\frac{V_{oc}}{mV_T}) \quad (8)$$

$$R_{sh} = R_{sho} \quad (9)$$

In order to give a sense of the accuracy of the method, Figure 5 shows the measured and modelled I-V curves for the modules under study at reference conditions. As can be seen, the method estimates the electrical output with a high quality. In particular, the maximum, minimum and average absolute percentage errors between actual and predicted power are, respectively, 0.12%, 0.01% and 0.05% for module A, and 0.10%, 0.01% and 0.07% for module B. This accuracy is important to be confident with the results obtained and discussed below.

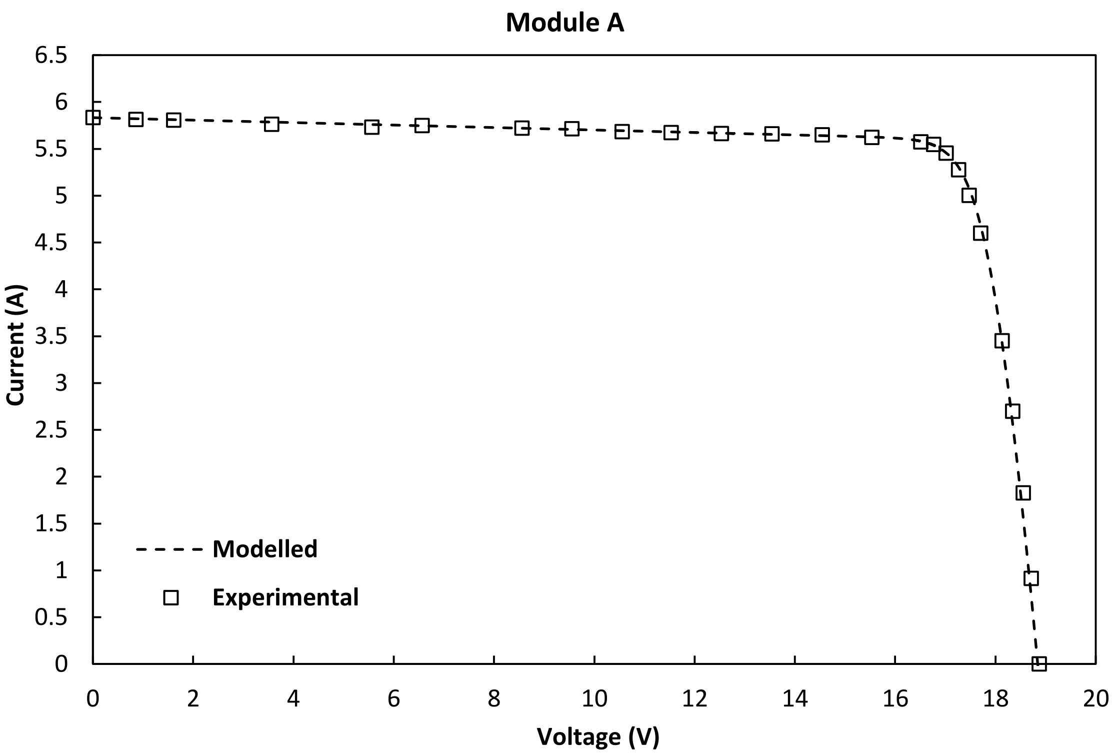

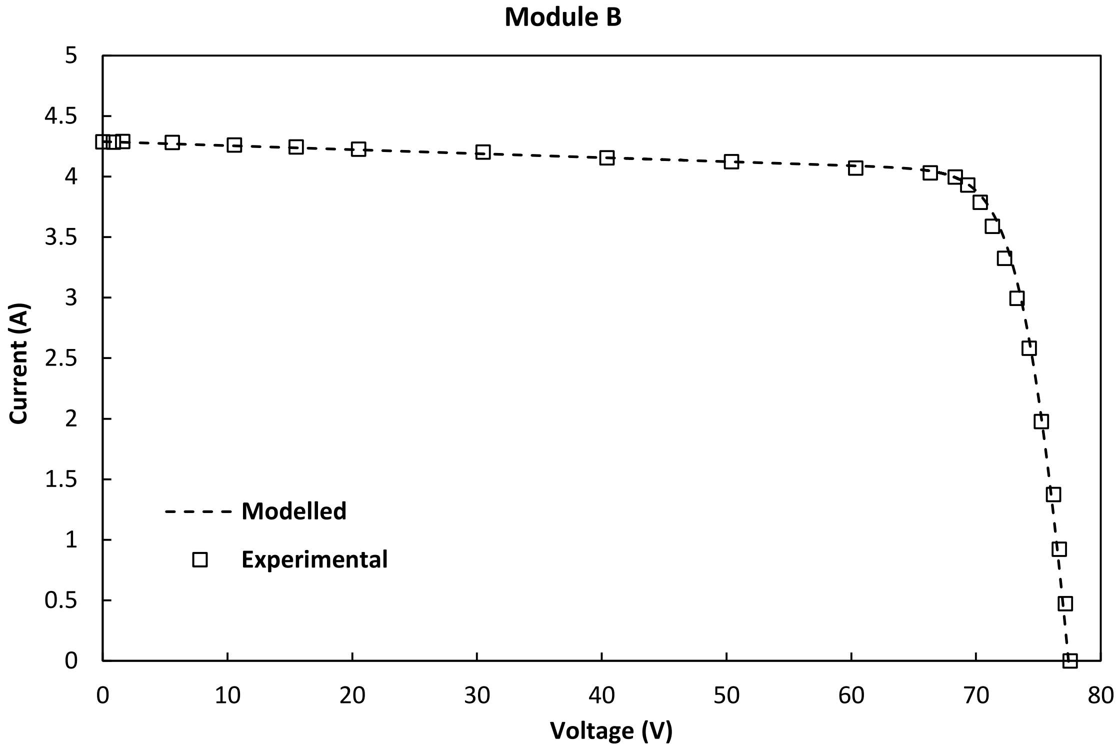

Figure 5. Experimental and modelled current-voltage curve of the CPV modules used in this study at 1000 W/m[2], spectral irradiance similar to AM1.5D reference spectrum, SMR (top/mid) = 1 ± 0.05 and room temperature of 25ºC ± 0.5ºC.

3.2. Results

In this section, the dependence of the SEM model parameters of the modules with light intensity is discussed. It should be noted that the parameters are given and discussed at one-cell level by considering the electrical configuration of the modules as:

$$I_{ph,c} = I_{ph} \quad (10)$$

$$I_{o,c} = I_o \quad (11)$$

$$m_c = \frac{m}{N_s} \quad (12)$$

$$R_{s,c} = \frac{R_s}{N_s} \quad (13)$$

$$R_{sh,c} = R_{sh} \quad (14)$$

where the subscript "c" refers to the values at cell level and N_s the number of cells in series of each module. The use of normalized values is more appropriate since allows the extracted values of both modules to be directly compared. In addition, this also allows the results to be discussed based on previous studies concerning MJ solar cells. Moreover, the values provided can be easily translated to other modules by considering the specific number of cells in series of the specific concentrator considered.

Table 3 shows the extracted parameters of the CPV modules under study at reference conditions. As can be seen, the module A has a higher value of $I_{ph,c}$ than the module B, around 1.35 times greater, due to the its larger cell area. On the contrary, the module A presents a much lower value of $I_{o,c}$ than the module B, an order of magnitude around 4E+5 times. Regarding the ideality factor, the module B has a higher value, around 1.20 times greater than module A. Both modules present a similar value of $R_{s,c}$, while they present a significant difference for $R_{sh,c}$, a value around 4 times greater for the module B.

Parameter	**Module A**	**Module B**
$I_{ph,c}$ (A)	5.84	4.30
$I_{o,c}$ (A)	9.43E-25	4.11E-19
m_c	3.14	3.76
$R_{s,c}$ (Ω)	1.91E-02	1.93E-02
$R_{sh,c}$ (Ω)	75.9	302.5

Table 3. Single exponential model parameters of the CPV modules used in this study at 1000 W/m^2, spectral irradiance similar to AM1.5D reference spectrum, SMR (top/mid) = 1 ± 0.05 and room temperature of 25ºC ± 0.5ºC. The values of the parameters are given at one-cell level by considering the electrical configuration of the modules.

Figure 6-top shows the evolution of $I_{ph,c}$ with light intensity for the two modules considered. Under uniform irradiance, the photo-generated current of multi-junctions solar cells is expected to have a linear behaviour with intensity (Kinsey, et al., 2008). However, the assembly of concentrator optics affects the spatial and spectral distribution of the irradiance over the solar cells surface (Victoria, et al., 2013) and produce intrinsic electrical mismatches among the receivers (Vorster & Van Dyk, 2005), which can affect the behaviour of $I_{ph,c}$. Despite the possible effect of these phenomena, the extracted values of $I_{ph,c}$ are largely dominated by intensity and show a clear linear tendency with irradiance for both modules. They range from a value of 4.27 A (700 W/m^2) to 5.84 A (1000 W/m^2) for the module A, and from a value of 3.03 A (700 W/m^2) to 4.30 A (1000 W/m^2) for the module B. It should be noted that this linear behaviour, R^2 = 0.99 for both modules, also verifies the negligible effect on the results of the narrow spectral variations commented in section 2.

Figure 6-mid shows the values of ln($I_{o,c}$) and m_c as a function of the input irradiance for the two sample modules. These two parameters provided information about the rate and type of recombination mechanism that occurs in the solar cells (i.e. Radiative, Auger and Shockley-Read-Hall) (Nelson, 2014). Hence, they are expected to be sensible to the incident irradiance since this affects the injection level. As is shown, the extracted values of ln($I_{o,c}$) and m_c present a similar behaviour and do not show any particular trend with irradiance. The ln($I_{o,c}$) range from a value of -58.4 A (900 W/m^2) to -51.3 A (800 W/m^2) for the module A, and from a value of -50.5 A (800 W/m^2) to -42.6 A (700 W/m^2) for the module B. Also, the m_c values range from a minimum of 3.0 (900 W/m^2) to a maximum of 3.3 (800 W/m^2) for the module A, and from a minimum of 3.3 (800 W/m^2) to a maximum of 3.8 (700 W/m^2) for the module B. Based on these results, it can be concluded that the recombination processes of the solar cells are not significantly affected by intensity variations. In addition, the module A shows an average value of m_c of 3.2, around 1.0 per subcell, and the module B shows an average value of m_c of 3.6, around 1.2 per subcell. So, the conversion of photons into electricity of the multi-junction solar cells of both modules, for the

irradiance levels considered, seems to be dominated by radiative recombination in the surface and bulk region (Siefer & Bett, 2014).

Figure 6-bottom shows the dependence of parasitic resistances, i.e. $R_{s,c}$ and $R_{sh,c}$, with irradiance variations. The $R_{s,c}$ of a solar cell is mainly determined by the resistance of the semiconductor layers, by the front metal grid resistance and by the metallic contact resistance (Vossier, et al., 2012). In this case, the $R_{s,c}$ is also going to be affected by the resistance of the wires of the CPV modules. As can be seen, the $R_{s,c}$ trends to decrease with intensity for both modules. It ranges from a value of around 0.023 Ω (700 W/m^2) to 0.019 Ω (1000 W/m^2). This tendency can be understood by considering the increase of the conductivity of the semiconductor layers with the number of charge carriers, and therefore, with the input irradiance (Grundmann, 2010). This trend can be approximated with the following equation:

$$R_{s,c} = a_{Rs} exp(-b_{Rs} DNI) \tag{15}$$

with an R^2 around 0.80 for both modules. The $R_{s,c}$ of a GaInP/GaAs/Ge solar cell has previously proven to decrease with concentration and ranges from a value of around 0.016 Ω (350 suns) to 0.009 Ω (900 suns) at 25ºC (Ben Or & Appelbaum, 2014). As expected, these values are slightly lower than the reported for the two CPV modules, probably due to the contribution of the resistance of the wires. Despite of this, it can be stated that the evolution of $R_{s,c}$ with light intensity is dominated by the dependence of the properties of the semiconductor materials.

On the other hand, the $R_{sh,c}$ is usually attributed to manufacturing defects that produce a leakage current flowing through the solar cell and around the edges of the semiconductor device (Nelson, 2014). In the case of concentrator modules, the extracted values of $R_{sh,c}$ are also going to be affected by possible optical and electrical mismatches among the receivers. As shown in Figure 6-bottom, the $R_{sh,c}$ shows a clear tendency for diminishing with irradiance for both modules. It ranges from a value of 108.6 (700 W/m^2) to 75.9 (1000 W/m^2) for the module A, and from a value of 463.7 (700 W/m^2) to 302.5 (1000 W/m^2) for the module B. This trend can be explained due to the increase of the conductivity commented above, as well of the higher shunt leakage current as a function of the growing irradiance (Grundmann, 2010; Khan, et al., 2014). As in the previous case, this behaviour can be approximated with the following equation:

$$R_{sh,c} = a_{Rsh} exp(-b_{Rsh} DNI) \tag{16}$$

with an R^2 around 0.85 for both modules. The same tendency has been found for a GaInP/GaAs/Ge solar cell with $R_{sh,c}$ values raging from around 450 Ω (350 suns) to 160 Ω (900 suns) at 25ºC (Ben Or & Appelbaum, 2014). The results obtained for the module B are in agreement with these values, however, the module A presents significantly lower $R_{sh,c}$ values. This could be explained due to the possible decrease of the slope of the I-V curves near short-circuit current by the presence of optical mismatches (Vorster & Van Dyk, 2005). Despite of this effect, the dependence of $R_{sh,c}$ with irradiance has demonstrated to be dominated by the changes of the properties of the semiconductors materials.

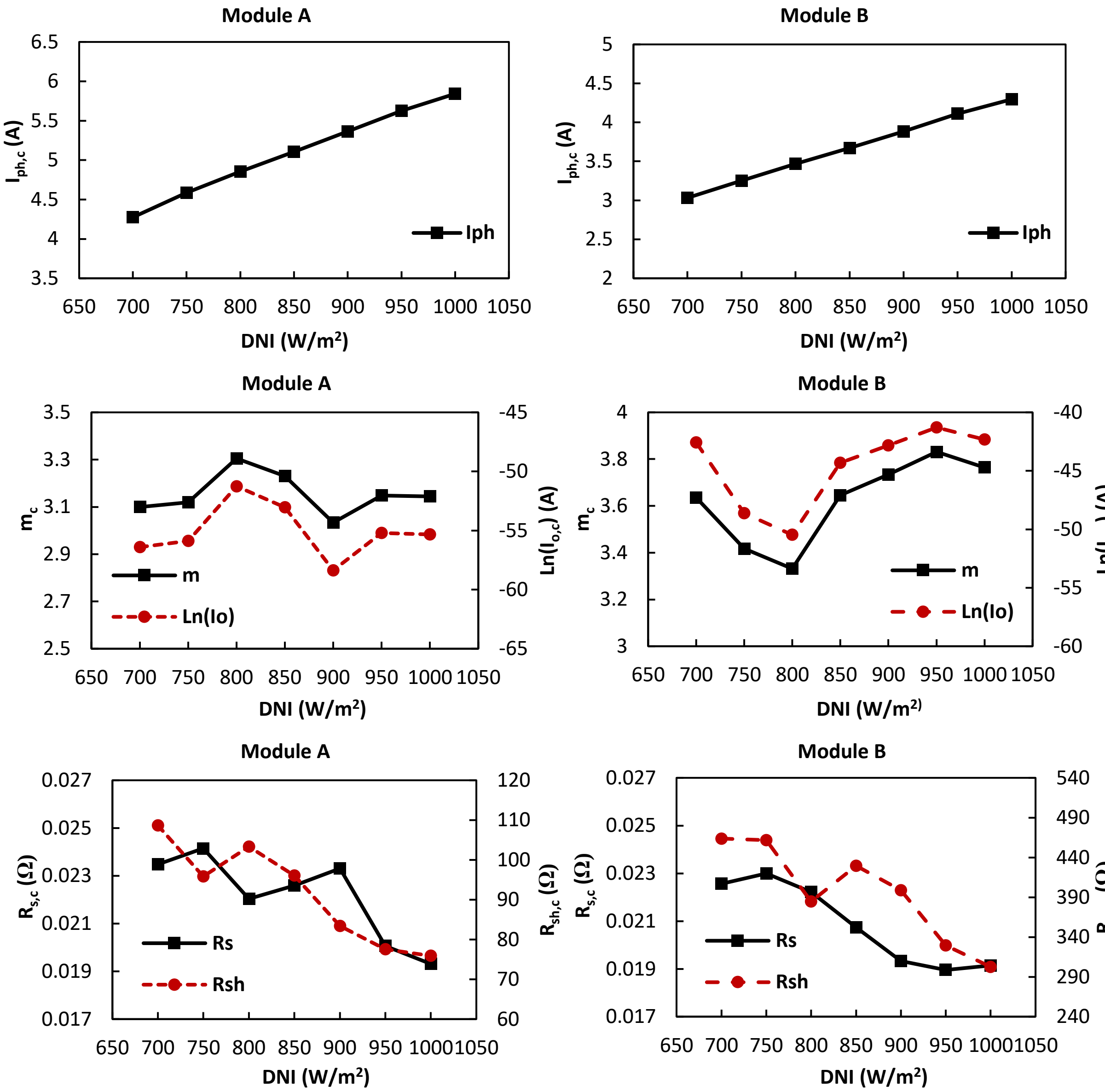

Figure 6. Dependence of single exponential model parameters with input irradiance of the CPV modules under study. The values of the parameters are given at one-cell level by considering the electrical configuration of the module.

4. Dependence of I-V parameters with irradiance

Figure 7 shows the evolution of the key parameters of the I-V curves of both modules as a function of the input irradiance, namely, short-circuit current (I_{sc}), current at maximum power point (I_{mpp}), open-circuit voltage (V_{oc}) and voltage at maximum power point (V_{mpp}). Based on the results obtained in the previous section, different approximations are carried out in the SEM model to explain the results found.

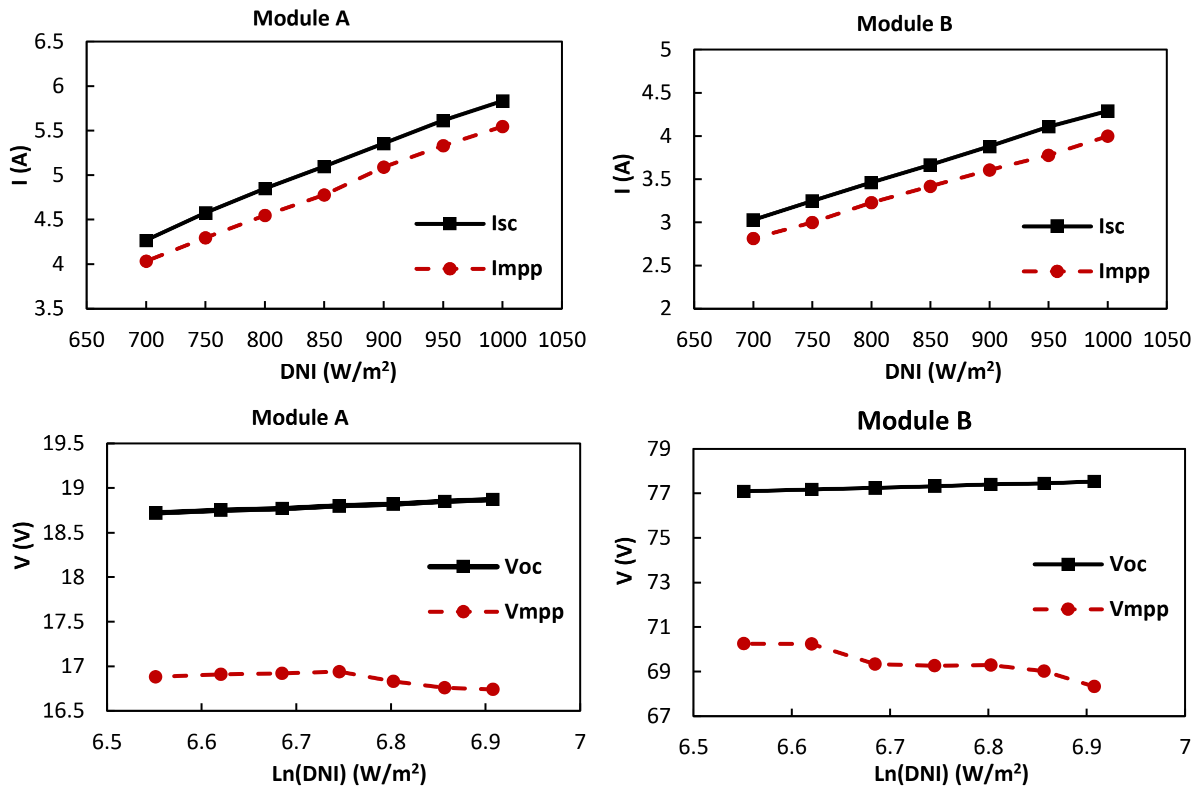

Figure 7. Dependence of current-voltage parameters with input irradiance of the CPV modules under study.

As shown in Figure 7-top, I_{sc} presents a clear linear tendency with irradiance for both modules. This can be explained by setting V = 0 in Equation (1) at reference conditions, "*", as follows:

$$I_{sc}^{*} = I_{ph}^{*} - I_{o}^{*}\left(\exp\left(\frac{I_{sc}^{*}R_{s}^{*}}{m^{*}V_{T}}\right) - 1\right) - \frac{I_{sc}^{*}R_{s}^{*}}{R_{sh}^{*}} \approx I_{ph}^{*} \quad (17)$$

Then, under different irradiance levels, I_{sc} can be expressed with the following:

$$I_{sc} \approx \frac{I_{ph}^{*}}{DNI^{*}}DNI \approx \frac{I_{sc}^{*}}{DNI^{*}}DNI \quad (18)$$

As in the previous case, I_{mpp} shows a linear dependence with light intensity, see also Figure 7-top. This can be understood by setting V = V_{mpp} and I = I_{mpp} and rearranging Equation (1) at reference conditions as:

$$I_{ph}^{*} = I_{mpp}^{*} + I_{o}^{*}\left(\exp\left(\frac{V_{mpp}^{*}+I_{mpp}^{*}R_{s}^{*}}{m^{*}V_{T}}\right) - 1\right) + \frac{V_{mpp}^{*}+I_{mpp}^{*}R_{s}^{*}}{R_{sh}^{*}} \quad (19)$$

With light intensity, I_{mpp} can be expressed as follows:

$$I_{mpp} = \frac{I_{ph}^{*}}{DNI^{*}}DNI - I_{o}\left(\exp\left(\frac{V_{mpp}+I_{mpp}R_{s}}{mV_{T}}\right) - 1\right) - \frac{V_{mpp}+I_{mpp}R_{s}}{R_{sh}} \quad (20)$$

After substituting I_{ph}^{*} in this equation, I_{mpp} can be simplified to the following expression:

$$I_{mpp} \approx \frac{I_{mpp}^{*}}{DNI^{*}} DNI \tag{21}$$

Based on the above, it could be stated that I_{sc} and I_{mpp} present the same behaviour than I_{ph} with intensity variations and that are not significantly affected by the presence of parasitic resistances.

Figure 7-bottom shows the evolution of V_{oc} with the intensity of the light. As shown, V_{oc} grows with a logarithmic dependence as the irradiance increases. According to Equation (1), at reference conditions, V_{oc} (I = 0) can be expressed as:

$$V_{oc}^{*} = m^{*} V_T ln\left(\frac{I_{ph}^{*}}{I_o^{*}} - \frac{V_{oc}^{*}}{R_{sh}^{*} I_o^{*}} + 1\right) \approx m^{*} V_T ln\left(\frac{I_{ph}^{*}}{I_o^{*}}\right) \tag{22}$$

Based on this, under irradiance variations, V_{oc} can be approximated to the following expression:

$$V_{oc} \approx m V_T ln\left(\frac{DNI}{DNI^{*}} \frac{I_{ph}^{*}}{I_o^{*}}\right) \approx V_{oc}^{*} + m V_T \ln(\frac{DNI}{DNI^{*}}) \tag{23}$$

Hence, it could also be considered independent of parasitic resistances. In addition, the slope of V_{oc} as a function of ln(DNI) shows a constant behaviour. This confirms the narrow dependence of the ideality factor of the modules with irradiance commented in the previous section.

Figure 7-bottom also shows the evolution of V_{mpp} with light intensity. This parameter has proven a more complex dependence than the previous. It trends to grow with ln(DNI) until a certain level and then starts to decrease gradually due to series resistance losses. This can also be explained from Equation (1) following different approximations. At maximum power, V_{mpp} at reference conditions can be expressed as:

$$V_{mpp}^{*} = m^{*} V_T ln\left(\frac{I_{ph}^{*} - I_{mpp}^{*}}{I_o^{*}} - \frac{V_{mpp}^{*} + I_{mpp}^{*} R_S^{*}}{R_{sh}^{*} I_o^{*}} + 1\right) - I_{mpp}^{*} R_S^{*} \approx m^{*} V_T ln\left(\frac{I_{ph}^{*} - I_{mpp}^{*}}{I_o^{*}}\right) - I_{mpp}^{*} R_S^{*} \tag{24}$$

So, with light intensity, V_{mpp} can be approximated to the following equation:

$$V_{mpp}(DNI) \approx m V_T ln\left(\frac{DNI}{DNI^{*}} \frac{I_{ph}^{*} - I_{mpp}^{*}}{I_o^{*}}\right) - \frac{DNI}{DNI^{*}} I_{mpp}^{*} R_s \approx V_{mpp}^{*} + m V_T ln\left(\frac{DNI}{DNI^{*}}\right) - I_{mpp}^{*} R_s (\frac{DNI}{DNI^{*}} - 1) \tag{25}$$

This analysis demonstrates that the behaviour of V_{oc} and V_{mpp} is dominated by ln(DNI) variations. However, despite the reduction of R_s with irradiance, it causes V_{mpp} to decrease above a certain irradiance level. The presence of R_{sh} does not play a relevant role on the performance of these two parameters.

It should be noted that, based on the experimental data and relationships described above, the behaviour of the parameters with irradiance shown in Figure 7 can be approximated with the following simple expressions:

$$I_{sc} \approx a \cdot DNI \tag{26}$$

$$I_{mpp} \approx b \cdot DNI \tag{27}$$

$$V_{oc} \approx c_1 ln(DNI) + c_2 \tag{28}$$

$$V_{mpp} \approx d_1 ln(DNI) - d_2 \cdot DNI + d_3 \tag{29}$$

with a high quality - a R^2 within 0.95-0.99 for both modules. In order show an example of the high accuracy of these approximations, Figure 8 shows the measured and modelled V_{mpp}, the parameter with the more complex behaviour, for the module A. These approximations are useful since avoid the SEM model parameters and the I-V characteristics under reference conditions to be known. Hence, they offer a simple and accurate way for predicting the main electrical parameters as a function of the irradiance by performing simple regression analysis from monitored data.

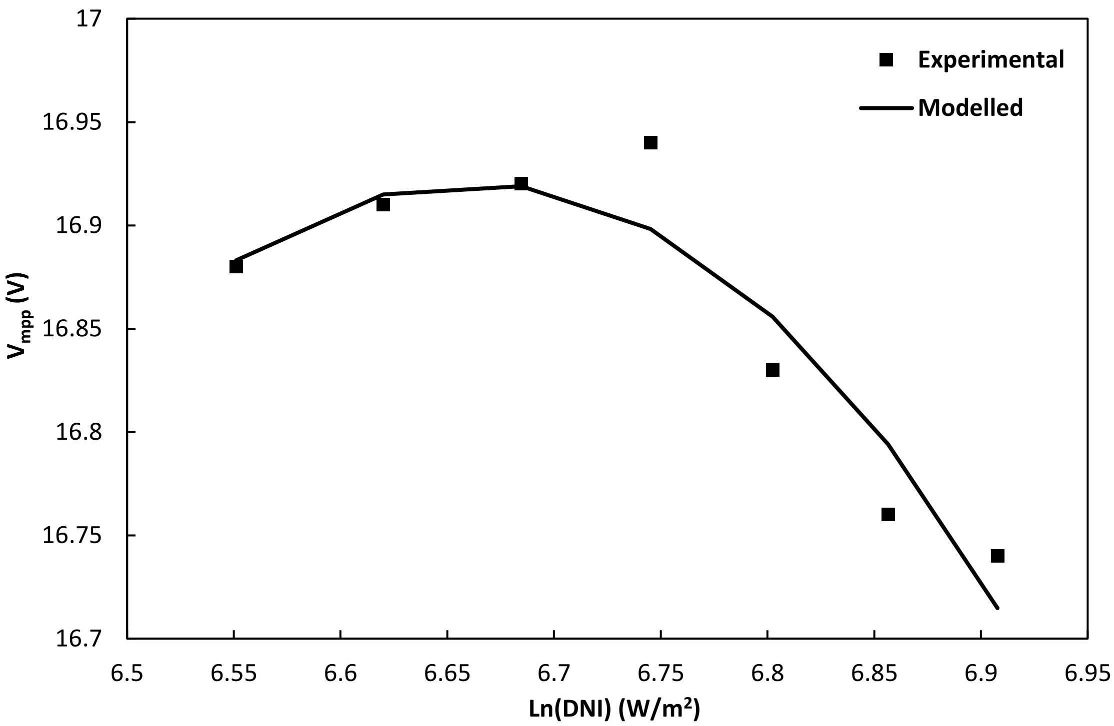

Figure 8. Experimental versus modelled voltage at maximum power point (V_{mpp}) as a function of the incident irradiance for the module A.

The outcome of this study also indicates that the performance of the CPV modules is going to be limited by the effect of R_s on V_{mpp}. The fill factor (FF) of a photovoltaic device can be written as:

$$FF = \frac{I_{mpp}V_{mpp}}{I_{sc}V_{oc}} \tag{30}$$

By combining Equations (18), (21), (23) and (25), FF can be rewritten as:

$$FF = \frac{I_{mpp}^*}{I_{sc}^*}\frac{V_{mpp}^* + mV_T ln\left(\frac{DNI}{DNI^*}\right) - I_{mpp}^* R_S(\frac{DNI}{DNI^*} - 1)}{V_{oc}^* + mV_T \ln(\frac{DNI}{DNI^*})} \quad (31)$$

So, FF trends to unity as the irradiance increases without considering the effect of series resistance. However, for real concentrators, it tends to diminish above a determined irradiance level due to the increase of $R_s \cdot DNI/DNI^*$.

The efficiency (η) of a concentrator module can be expressed by means of the following equation:

$$\eta = \frac{P_{mpp}}{A_{module} DNI} \quad (32)$$

where P_{mpp} is the maximum power and A_{module} is the area of the concentrator. By combining Equations (18), (23) and (30), η can be rewritten as:

$$\eta = \frac{I_{sc}^*}{A_{module} DNI^*}(V_{oc}^* + mV_T \ln(\frac{DNI}{DNI^*}))FF \quad (33)$$

Hence, the efficiency of the modules trends to grow due to the logarithmic increase of V_{oc} with the intensity of the light. However, as the irradiance increases, this effect is counterbalanced by the decrease of FF due to series losses. As a result, η of the modules decreases above a certain level.

The effect of the series resistance on FF and η with the increase of the intensity of the light is shown in Figure 9. The FF decreases around 1% and 3% for the module A and B respectively. Regarding η, it is reduced approximately 1% for both modules. It is worth mentioning that the maximum of FF and η with irradiance cannot be clearly identified since it could happen at lower irradiance levels than the considered in this study. This highlights the importance of the coupling between the concentration of the modules and the peak of efficiency of the cells. The geometry and properties of the optical elements need to be carefully selected and designed to ensure multi-junction solar cells to operate around their maximum efficiency for the typical irradiance levels in outdoors. In addition, the reduction of the series resistance of the modules seems to be a crucial concern to have a peak efficiency at higher irradiance levels, and therefore, to maximize the energy harvested by CPV systems under real working conditions.

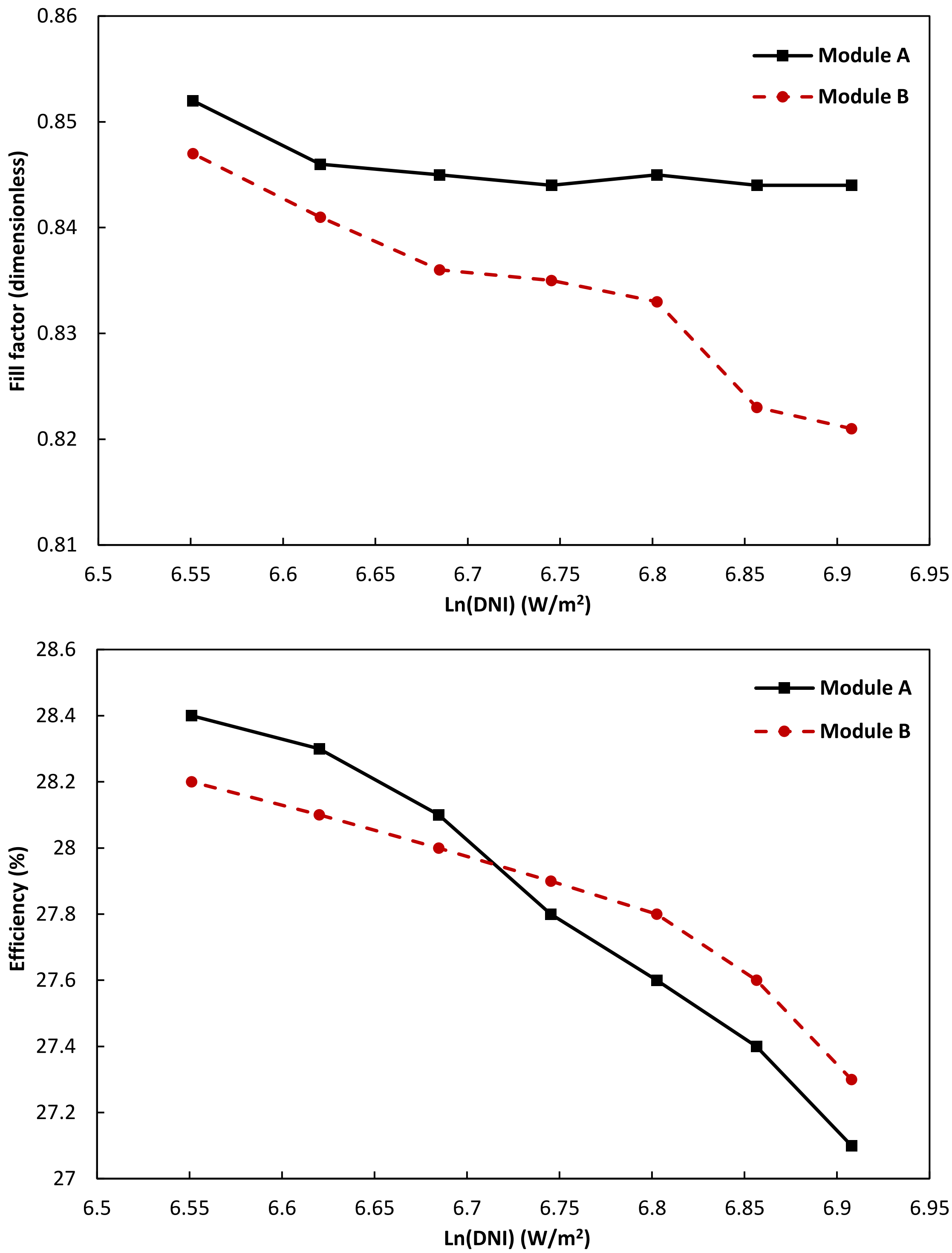

Figure 9. Dependence of fill factor and efficiency with input irradiance of the CPV modules under study.

5. Modelling the electrical characteristics from reference values

The analysis and relationships discussed in the previous sections allow the electrical characteristics of concentrator PV modules as a function of the incident irradiance to be understood. For electrical modelling purposes, it is interesting to evaluate the accuracy in the estimation of the I-V curve and key parameters from the values of the concentrators at reference conditions. This is useful since the electrical characteristics under standard conditions are the variables provided by the manufacturers and testing laboratories in the majority of the cases. Hence, they are the only magnitudes available when is not possible to perform long-term outdoor measurements or to use a solar simulator able to change the input irradiance.

Figure 10 shows an example of the measured and modelled I-V curve for the module A and the relative error between actual and predicted maximum power as a function of the input intensity for both modules. The photo-generated current at each light intensity has been estimated from the reference values, considering the linear dependency discussed in section 3, with the following equation:

$$I_{ph} \approx \frac{I_{ph}^*}{DNI^*} DNI \qquad (34)$$

The rest of the parameters of the SEM model equation have been kept constant at the values given in table 3 and considering the number of cell in series of each module. As can be seen, the error in the fitting of the I-V curves increases as the irradiance decreases. Despite of this, this approximation offers a good quality for both modules until irradiance values around 750 W/m^2 due to the fact that the absolute percentage error in the estimation of the maximum power is below 0.3%. So, it can be considered as a good first approximation to predict the I-V curve of concentrator modules for the typical operating irradiance levels in outdoors when the dependencies of the parameters of the SEM equation are unknown.

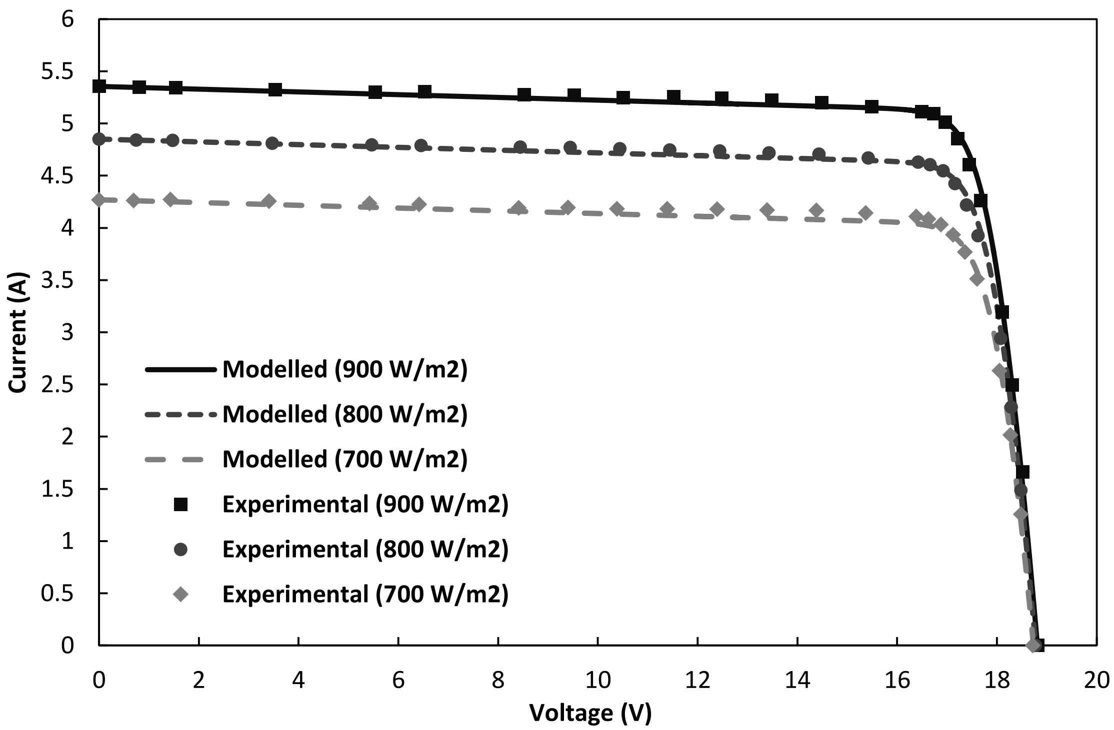

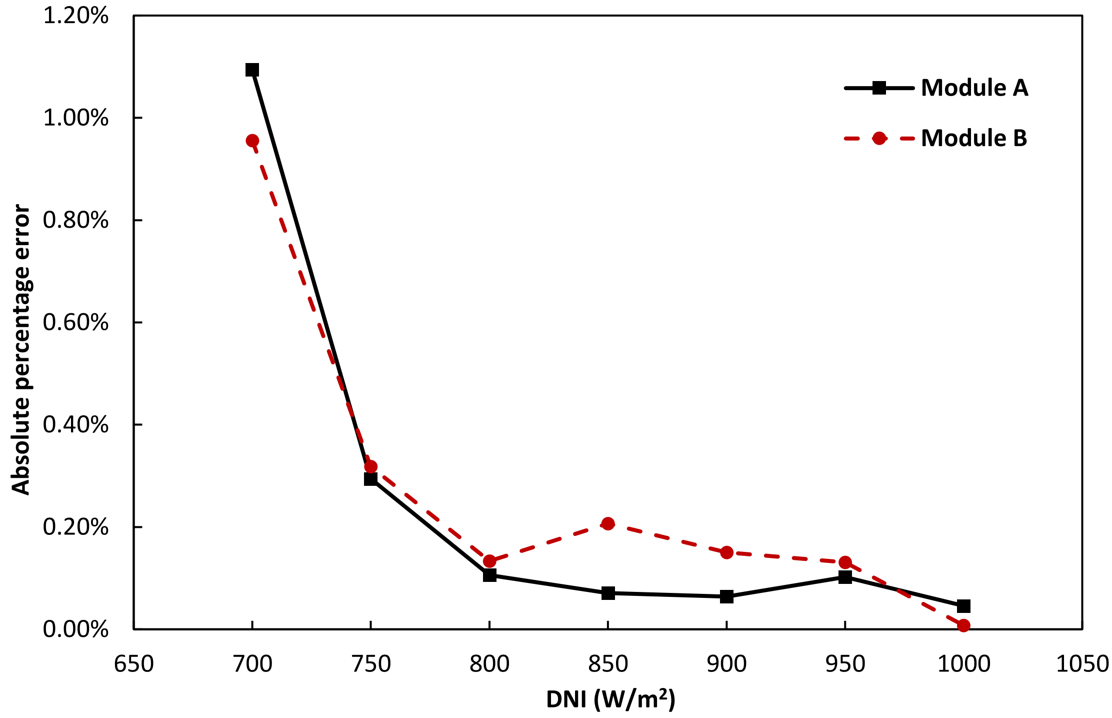

Figure 10. Top: Experimental and modelled current-voltage curve by using the reference values of the CPV module A at three different irradiance levels, spectral irradiance similar to AM1.5D reference spectrum, SMR (top/mid) = 1 ± 0.05 and room temperature of 25ºC ± 0.5ºC. Bottom: Absolute percentage error between actual and estimated maximum power by using the reference values as a function of the direct normal irradiance (DNI) of the CPV modules used in this study.

For the same reasons above, it is interesting to evaluate the accuracy in the estimation of the key electrical parameters of the modules from the reference values. These parameters have been estimated by means of equations (18), (21), (23) and (25) and the reference values provided in Tables 2 and 3. Different statistical parameters have been calculated: the mean absolute percentage error (MAPE), the mean relative error (MRE) and the determination coefficient (R^2). These magnitudes have been calculated by means of the following expressions:

$$MAPE\ (\%) = \frac{100}{N}\sum_{i=1}^{N}\left|\frac{Z_{modelled}-Z_{measured}}{Z_{measured}}\right| \tag{35}$$

$$MRE\ (\%) = \frac{100}{N}\sum_{i=1}^{N}\frac{Z_{modelled}-Z_{measured}}{Z_{measured}} \tag{36}$$

$$R = \frac{\sum_{i=1}^{N}(Z_{measured}-\overline{Z_{measured}})(Z_{modelled}-\overline{Z_{modelled}})}{\sqrt{\sum_{i=1}^{N}(Z_{measured}-\overline{Z_{measured}})^2\sum_{i=1}^{N}(Z_{modelled}-\overline{Z_{modelled}})^2}} \tag{37}$$

Where N is the number of samples and Z represents the electrical parameter considered.

As can be seen in table 4, the proposed approximations present a low variation of the estimated data around the experimental with a maximum MAPE of 1.2%. Also, the MRE is within 1%, which indicates that the approximations neither overestimate nor underestimate the electrical parameters significantly. Finally, a close match between actual and predicted data has been found – an R^2 equal of higher than 0.9.

	Module A			Module B		
Parameter	**MAPE (%)**	**MRE (%)**	**R^2**	**MAPE (%)**	**MRE (%)**	**R^2**
I_{sc}	1.2	0.4	0.98	0.4	0.4	0.99
I_{mpp}	1.1	1.0	0.99	0.3	0.2	0.99
V_{oc}	0.0	0.0	0.99	0.0	0.0	0.99
V_{mpp}	0.1	0.0	0.90	0.3	0.0	0.90

Table 4. Mean absolute percentage error (MAPE), mean absolute error (MRE) and determination coefficient (R^2) between actual and predicted electrical parameters of the CPV modules under study using Equations (11), (14), (16) and (18) and the values at reference conditions.

Bearing the above in mind, the use of the reference values offer a simple way to predict the I-V curve and main electrical parameters of multi-junction CPV modules for the typical irradiance levels with a low margin of error. Obviously, under real operating conditions, thermal and spectral corrections need to be incorporated to model the electrical output with a satisfactory degree of accuracy. This should be the topic of next research activities concerning this issue.

6. Conclusions

This paper is focused on the analysis of the current-voltage output of multi-junction CPV modules under different irradiance levels. To carry out this study, two samples of concentrator modules were experimentally characterized in indoor laboratory at the CEAEMA of the University of Jaen by using the Helios 3198 CPV solar simulator. The I-V curves of both systems were recorded for light intensities within 700-1000 W/m^2, spectral irradiance similar to AM1.5D reference spectrum, SMR (top/mid) = 1 ± 0.05 and room temperature of 25ºC ± 0.5ºC. Based on these data, the single exponential model (SEM) parameters and I-V characteristics of the modules as a function of the input irradiance were extracted and discussed.

Results show that the photo-generated current increases linearly with irradiance. The diode ideality factor and saturation current have proven a noteworthy stable behaviour under irradiance variations. On the contrary, the parasitic resistances, i.e. series and shunt, of both concentrators have shown a clear tendency to decrease as the intensity increases. The fundamentals behind the behaviour of the SEM model parameters of the CPV modules are also discussed in relation to the physical properties of the multi-junction solar cells of the concentrators. In addition, different approximations are carried out in the I-V characteristic equation to explain the dependence of the electrical output of the devices with light intensity. Results show that the short-circuit current (I_{sc}) and current at maximum power point (I_{mpp}) are not affected by parasitic resistances and increase with a linear behaviour with irradiance. On the other hand, the open-circuit voltage (V_{oc}) and voltage at maximum power point (V_{mpp}) have proven to grow with a logarithmic dependence as the irradiance increases. However, while V_{oc} can be considered independent of parasitic resistances, V_{mpp} has demonstrated to decrease above a certain light intensity due to the increase of series resistance losses. Finally, the accuracy in the estimation of I-V curves and key electrical parameters of the concentrators from reference values are investigated. Results show that the I-V curves can be modelled with a good quality until irradiance values of around 750 W/m^2 due to an error in the estimation of the maximum power below 0.3%. The modelling of the main electrical parameters, i.e. I_{sc}, I_{mpp}, V_{oc} and V_{mpp}, present a high quality with a mean percentage absolute error (MAPE) lower than 1.2%, a mean relative error (MRE) within 1% and a determination coefficient (R^2) equal of higher than 0.9.

Future works should study the impact of temperature on the performance of the SEM model parameters and the I-V characteristics under different irradiance levels. This is a crucial next step to leverage our understanding of the electrical output of CPV modules under real working conditions. In addition, the validation of the relationships to predict the electrical parameters should be extended to a wider irradiance range to ensure their accuracy for low irradiance conditions. Thermal and spectral corrections have to be also incorporated with the aim of modelling the current-voltage output under the relevant time-varying atmospheric variables in outdoors.

Acknowledges

Eduardo F. Fernández acknowledges the Spanish Ministry of Economy and Competitiveness for the Juan de la Cierva 2013 and 2015 fellowships. The authors also thank the Spanish Ministry of Economy and Competitiveness and FEDER funds for the projects ENE2013-45242-R and ENE2016-78251-R, and the "Plan de Apoyo a la Investigación de la Universidad de Jaén y la Caja Rural de Jaén" (UJA2015/07/01).

References

Almonacid, F., Rodrigo, P. & Fernández, E. F., 2016. Determination of the current-voltage characteristics of concentrator systems by using different adapted conventional techniques. *Energy,* Volume 101, pp. 146-160.

Almonacid, F., Rodrigo, P. & Fernández, E. F., 2016. Determination of the current–voltage characteristics of concentrator systems by using different adapted conventional techniques. *Energy,* Volume 101, p. 46–160.

Appelbaum, J. & Peled, A., 2014. Parameters extraction of solar cells - A comparative examination of three methods. *Solar Energy Materials and Solar Cells,* Volume 122, pp. 164-173.

Baig, H., Heasman, K. & Mallick, T., 2012. Non-uniform illumination in concentrating solar cells. *Renewable and Sustainable Energy Reviews,* 16(8), pp. 5890-5909.

Ben Or, A. & Appelbaum, J., 2013. Estimation of multi-junction solar cell parameters. *Progress in Photovoltaics: Research and Applications,* 21(4), pp. 713-723.

Ben Or, A. & Appelbaum, J., 2014. Dependence of multi-junction solar cells parameters on concentration and temperature. *Solar Energy Materials and Solar Cells,* Volume 130, pp. 234-240.

Ciulla, G., Lo Brano, V., Di Dio, V. & Cipriani, G., 2014. A comparison of different one-diode models for the representation of I-V characteristic of a PV cell. *Renewable and Sustainable Energy Reviews,* Volume 32, pp. 684-696.

Cotal, H. et al., 2009. III-V multijunction solar cells for concentrating photovoltaics. *Energy and Environmental Science,* 2(2), pp. 174-192.

Cotfas, D. T., Cotfas, P. A. & Kplanis, S., 2013. Methods to determine the dc parameters of solar cells: A critical review. *Renewable and Sustainable Energy Reviews,* Volume 28, pp. 588-596.

Domínguez, C., Antón, I. & Sala, G., 2008. Solar simulator for concentrator photovoltaic systems. *Optics Express,* 16(19), p. 14894–14901.

Domínguez, C., Antón, I. & Sala, G., 2010. Multijunction solar cell model for translating I-V characteristics as a function of irradiance, spectrum, and cell temperature. *Progress in Photovoltaics: Research and Applications,* 18(4), pp. 272-284.

Domínguez, C., Antón, I., Sala, G. & Askins, S., 2013. Current-matching estimation for multijunction cells within a CPV module by means of component cells. *Progress in Photovoltaics: Research and Applications,* 21(7), pp. 1478-1488.

Fernández, E., Almonacid, F., Rodrigo, P. & Pérez-Higueras, P., 2013b. Model for the prediction of the maximum power of a high concentrator photovoltaic module. *Solar Energy,* Volume 97, pp. 12-18.

Fernández, E., Almonacid, F., Ruiz-Arias, J. & Soria-Moya, A., 2014. Analysis of the spectral variations on the performance of high concentrator photovoltaic modules operating under different real climate conditions. *Solar Energy Materials and Solar Cells,* Volume 127, pp. 179-187.

Fernández, E., Almonacid, F., Soria-Moya, A. & Terrados, J., 2015c. Experimental analysis of the spectral factor for quantifying the spectral influence on concentrator photovoltaic systems under real operating conditions. *Energy,* Volume 90, pp. 1878-1886.

Fernández, E. F., García-Loureiro, A. J. & Smestad, G. P., 2015a. Multijunction concentrator solar cells: Analysis and fundamentals. In: *High Concentrator Photovoltaics: Fundamentals, Engineering and Power Plants, Pérez-Higueras, Pedro and Fernández, Eduardo F. (Eds.).* s.l.:Springer, pp. 9-37.

Fernández, E. F. et al., 2016b. Comparative study of methods for the extraction of concentrator photovoltaic module parameters. *Solar Energy,* Volume 137, pp. 413-423.

Fernández, E. F., Talavera, D. L., Almonacid, F. M. & Smestad, G. P., 2016a. Investigating the impact of weather variables on the energy yield and cost of energy of grid-connected solar concentrator systems. *Energy,* Volume 106, pp. 790-801.

Fernández, E. et al., 2015b. Model for estimating the energy yield of a high concentrator photovoltaic system. *Energy,* Volume 87, pp. 77-85.

Fernández, E., Pérez-Higueras, P., Garcia Loureiro, A. & Vidal, P., 2013c. Outdoor evaluation of concentrator photovoltaic systems modules from different manufacturers: First results and steps. *Progress in Photovoltaics: Research and Applications,* 21(4), pp. 693-701.

Fernández, E. et al., 2013a. A two subcell equivalent solar cell model for III-V triple junction solar cells under spectrum and temperature variations. *Solar Energy,* Volume 92, pp. 221-229.

Fernández, E., Soria-Moya, A., Almonacid, F. & Aguilera, J., 2016c. Comparative assessment of the spectral impact on the energy yield of high concentrator and conventional photovoltaic technology. *Solar Energy Materials and Solar Cells,* Volume 147, pp. 185-197.

Ghani, F., Fernandez, E., Almonacid, F. & O'Donovan, T., 2017. The numerical computation of lumped parameter values using the multi-dimensional Newton-Raphson method for the characterisation of a multi-junction CPV module using the five-parameter approach. *olar Energy,* Volume 149, pp. 302-313.

Ghani, F., Rosengarten, G., Duke, M. & Carson, J., 2014. The numerical calculation of single-diode solar-cell modelling parameters. *Renewable Energy,* Volume 72, pp. 105-112.

Grundmann, M., 2010. *The Physics of Semiconductors.* s.l.:Springer Berlin Heidelberg.

Humada, A., Hojabri, M., Mekhilef, S. & Hamada, H., 2016. Solar cell parameters extraction based on single and double-diode models: A review. *Renewable and Sustainable Energy Reviews,* Volume 56, pp. 494-509.

Khan, F., Baek, S. & Kim, J., 2014. Intensity dependency of photovoltaic cell parameters under high illumination conditions: An analysis. *Applied Energy,* Volume 133, pp. 356-362.

Kim, Y., Kang, S.-M. & Winston, R., 2013. Modeling of a concentrating photovoltaic system for optimum land use. *Progress in Photovoltaics: Research and Applications,* 21(2), pp. 240-249.

Kinsey, G. et al., 2008. Concentrator multifunction solar cell characteristics under variable intensity and temperature. *Progress in Photovoltaics: Research and Applications,* 16(6), pp. 503-508.

Kurtz, S. et al., 2015. Key parameters in determining energy generated by CPV modules. *Progress in Photovoltaics: Research and Applications,* 23(10), pp. 1250-1259.

Leloux, J. et al., 2014. A bankable method of assessing the performance of a CPV plant. *Applied Energy,* Volume 118, pp. 1-11.

Li, W. et al., 2016. Six-parameter electrical model for photovoltaic cell/module with compound parabolic concentrator. *Solar Energy,* Volume 137, pp. 551-563.

Li, Y. et al., 2013. Evaluation of methods to extract parameters from current-voltage characteristics of solar cells. *Solar Energy,* Volume 90, pp. 51-57.

Micheli, L. et al., 2016. Performance, limits and economic perspectives for passive cooling of High Concentrator Photovoltaics. *Solar Energy Materials and Solar Cells,* Volume 153, p. 164–178.

Muller, M., Kurtz, S., Steiner, M. & Siefer, G., 2015. Translating outdoor CPV I-V measurements to a CSTC power rating and the associated uncertainty. *Progress in Photovoltaics: Research and Applications,* 23(11), pp. 1557-1571.

Nelson, J., 2014. *The Physics of Solar Sells.* London: Imperial College Press.

Peharz, G., Ferrer-Rodríguez, J., Siefer, G. & Bett, A., 2011. A method for using CPV modules as temperature sensors and its application to rating procedures. *Solar Energy Materials and Solar Cells,* 95(10), pp. 2734-2744.

Peharz, G., Ferrer-Rodríguez, J., Siefer, G. & Bett, A., 2011. Investigations on the temperature dependence of CPV modules equipped with triple-junction solar cells. *Progress in Photovoltaics: Research and Applications,* 19(1), pp. 54-60.

Phang, J. C. H., Chan, D. S. H. & Phillips, J. R., 1984. Accurate analytical method for the extraction of solar cell model parameters. *Electronics letters,* 20(10), pp. 406-408.

Rodrigo, P., Fernández, E., Almonacid, F. & Pérez-Higueras, P., 2013. Models for the electrical characterization of high concentration photovoltaic cells and modules: A review. *Renewable and Sustainable Energy Reviews,* Volume 26, pp. 752-760.

Rodrigo, P., Fernández, E., Almonacid, F. & Pérez-Higueras, P., 2014. Review of methods for the calculation of cell temperature in high concentration photovoltaic modules for electrical characterization. *Renewable and Sustainable Energy Reviews ,* Volume 38, pp. 478-488.

Rodrigo, P., Micheli, L. & Almonacid, F., 2015. The high-concentrator photovoltaic module. In: *High Concentrator Photovoltaics: Fundamentals, Engineering and Power Plants. Perez-Higueras, P.; Fernández, Eduardo F. (Eds).* s.l.:springer, pp. 115-151.

Rodrigo, P. et al., 2016. Analysis of electrical mismatches in high-concentrator photovoltaic power plants with distributed inverter configurations. *Energy,* Volume 107, pp. 374-387.

Segev, G., Mittelman, G. & Kribus, A., 2012. Equivalent circuit models for triple-junction concentrator solar cells. *Solar Energy Materials and Solar Cells,* Volume 98, pp. 57-65.

Shanks, K. et al., 2016. Theoretical investigation considering manufacturing errors of a high concentrating photovoltaic of cassegrain design and its experimental validation. *Solar Energy,* Volume 131, pp. 235-245.

Siefer, G. & Bett, A., 2014. Analysis of temperature coefficients for III-V multi-junction concentrator cells. *Progress in Photovoltaics: Research and Applications,* 22(5), pp. 515-524.

Soria-Moya, A. et al., 2015. Performance Analysis of Models for Calculating the Maximum Power of High Concentrator Photovoltaic Modules. *IEEE Journal of Photovoltaics,* 5(3), pp. 947-955.

Steiner, M. et al., 2015. YieldOpt, a model to predict the power output and energy yield for concentrating photovoltaic modules. *Progress in Photovoltaics: Research and Applications,* 23(3), pp. 385-397.

Strobach, E. et al., 2015. Modeling a grid-connected concentrator photovoltaic system. *Progress in Photovoltaics: Research and Applications,* 23(5), pp. 582-592.

Talavera, D. et al., 2016. A worldwide assessment of levelised cost of electricity of HCPV systems. *Energy Conversion and Management,* Volume 127, pp. 679-692.

Talavera, D. L., Perez-Higueras, P. J., Almonacid, F. & Fernández, E. F., 2017. A worldwide assessment of economic feasibility of HCPV power plants: Profitability and competitiveness. *Energy,* Volume 119, p. 408–424.

Theristis, M., Fernández, E., Stark, C. & O'Donovan, T., 2016. A theoretical analysis of the impact of atmospheric parameters on the spectral, electrical and thermal performance of a concentrating III-V triple-junction solar cell. *Energy Conversion and Management,* Volume 117, pp. 218-227.

Theristis, M., Fernández, E., Sumner, M. & O'Donovan, T., 2017. Multiphysics modelling and experimental validation of high concentration photovoltaic modules. *Energy Conversion and Management,* Volume 129, pp. 122-134.

Theristis, M. & O'Donovan, T., 2015. Electrical-thermal analysis of III-V triple-junction solar cells under variable spectra and ambient temperatures. *Solar Energy,* Volume 118, pp. 533-546.

Victoria, M., Doḿinguez, C., Ant́on, I. & Sala, G., 2009. Comparative analysis of different secondary optical elements for aspheric primary lenses. *Optics Express,* 17(9), pp. 6487-6492.

Victoria, M. et al., 2013. Characterization of the spatial distribution of irradiance and spectrum in concentrating photovoltaic systems and their effect on multi-junction solar cells. *Progress in Photovoltaics: Research and Applications,* 21(3), pp. 308-318.

Vorster, F. & Van Dyk, E., 2005. Current-voltage characteristics of high-concentration, photovoltaic arrays. *Progress in Photovoltaics: Research and Applications,* 13(1), pp. 55-66.

Vossier, A., Chemisana, D., Flamant, G. & Dollet, A., 2012. Very high fluxes for concentrating photovoltaics: Considerations from simple experiments and modeling. *Renewable Energy,* Volume 38, p. 31–39.

Xie, W. T., Dai, Y., Wang, R. & Sumathy, K., 2011. Concentrated solar energy applications using Fresnel lenses: A review. *Renewable and Sustainable Energy Reviews,* 15(6), pp. 2588-2606.